Since January 2020 Elsevier has created a COVID-19 resource centre with free information in English and Mandarin on the novel coronavirus COVID-19. The COVID-19 resource centre is hosted on Elsevier Connect, the company's public news and information website.

Available online at www.sciencedirect.com

SCIENCE DIRECT

Virology 341 (2005) 122 – 129

VIROLOGY

www.elsevier.com/locate/yviro

Serine-scanning mutagenesis studies of the C-terminal heptad repeats in the SARS coronavirus S glycoprotein highlight the important role of the short helical region

Kathryn E. Follis, Joanne York, Jack H. Nunberg*

Montana Biotechnology Center, The University of Montana, Science Complex Room 221, Missoula, MT 59812, USA

Received 16 May 2005; returned to author for revision 28 June 2005; accepted 5 July 2005
Available online 2 August 2005

Abstract

The fusion subunit of the SARS-CoV S glycoprotein contains two regions of hydrophobic heptad-repeat amino acid sequences that have been shown in biophysical studies to form a six-helix bundle structure typical of the fusion-active core found in Class I viral fusion proteins. Here, we have applied serine-scanning mutagenesis to the C-terminal-most heptad-repeat region in the SARS-CoV S glycoprotein to investigate the functional role of this region in membrane fusion. We show that hydrophobic sidechains at ***a*** and ***d*** positions *only* within the short helical segment of the C-terminal heptad-repeat region (I1161, I1165, L1168, A1172, and L1175) are critical for cell–cell fusion. Serine mutations at outlying heptad-repeat residues that form an extended chain in the core structure (V1158, L1179, and L1182) do not affect fusogenicity. Our study provides genetic evidence for the important role of α-helical packing in promoting S glycoprotein-mediated membrane fusion.

Keywords: SARS; Coronavirus; Spike glycoprotein; Envelope glycoprotein; Membrane fusion; Six-helix bundle; Mutagenesis

Introduction

The emergence of the novel coronavirus responsible for the severe acute respiratory syndrome (SARS) in 2002–2003 (Drosten et al., 2003; Ksiazek et al., 2003; Kuiken et al., 2003; Marra et al., 2003; Peiris et al., 2003; Rota et al., 2003) highlights the public health risks associated with the continual evolution of human coronaviruses. The coronaviruses are a diverse family of enveloped, positive-sense RNA viruses that are distributed widely among animal species (Lai and Holmes, 2001). The major surface glycoprotein, the spike (S) glycoprotein, mediates the attachment of virions to the host-cell receptor and the subsequent fusion of the viral and cellular membranes. The S glycoprotein is also the target of neutralizing antibodies and a major determinant of pathogenicity (Lai and Holmes, 2001).

The coronavirus S glycoproteins share similarities with other Class I viral fusion proteins in their apparent use of a six-membered α-helical coiled-coil structure to promote fusion of the viral and cellular membranes (Bosch et al., 2003; Chambers et al., 1990). Class I viral fusion proteins, such as those of the retroviruses, filoviruses, orthomyxoviruses, and paramyxoviruses, contain two heptad-repeat regions, with a 3,4 periodicity in hydrophobic residues, that are poised to refold during virus entry to form a highly stable six-helix core (Eckert and Kim, 2001; Hughson, 1997; Skehel and Wiley, 2000; Weissenhorn et al., 1999, and references therein). In this structure, three α-helices formed by the C-terminal heptad repeats of the trimeric glycoprotein pack in an anti-parallel manner against conserved hydrophobic grooves on the surface of a central, three-stranded coiled coil formed by the N-terminal heptad repeats. Recent biophysical (Bosch et al., 2003; Ingallinella

* Corresponding author. Fax: +1 406 243 6425.
E-mail address: jack.nunberg@umontana.edu (J.H. Nunberg).

0042-6822/$ - see front matter © 2005 Elsevier Inc. All rights reserved.
doi:10.1016/j.virol.2005.07.005

et al., 2004; Liu et al., 2004; Tripet et al., 2004) and, specifically, crystallographic (Duquerroy et al., 2005; Supekar et al., 2004; Xu et al., 2004b) studies of the SARS-CoV S glycoprotein fusion domain have demonstrated a six α-helical core structure typical of Class I viral fusion proteins. In contrast to other viruses, however, only a short central portion of the SARS-CoV C-terminal heptad-repeat region assumes the α-helical form in the crystal structure (Fig. 1). The outlying heptad repeats appear as extended chains.

Considerable genetic and biophysical evidence supports the concept that the ability of the Class I envelope glycoprotein to mediate membrane fusion is determined, in part, by the stability of the six-helix bundle (Eckert and Kim, 2001; Hughson, 1997; Skehel and Wiley, 2000; Weissenhorn et al., 1999, and references therein). A general model for Class I viral protein-induced membrane fusion posits that the native envelope glycoprotein exists in a metastable state and, upon activation by receptor binding and/or endosomal pH, undergoes a structural reorganization that leads to exposure of the previously constrained fusion subunit and insertion of its hydrophobic "fusion peptide" into the cellular membrane. In this prehairpin intermediate, the fusion subunit is anchored to the viral membrane via its transmembrane domain and to the cellular membrane via the fusion peptide. Collapse of this intermediate leads to a trimer-of-hairpins structure in which the N- and C-terminal heptad-repeat regions assemble as anti-parallel α-helices to form the six-helix bundle, thereby bringing the viral and cellular membranes into apposition. The free energy made available through formation of the highly stable helical bundle is thought to drive fusion of the lipid bilayers. Thus, the kinetics and thermodynamics of six-helix bundle formation are critical determinants of envelope glycoprotein-mediated membrane fusion.

Here, we have utilized scanning mutagenesis to investigate amino acids at the repeating hydrophobic positions throughout the C-terminal heptad-repeat region of the S glycoprotein in order to assess their relative contributions in promoting membrane fusion. We show that serine mutations at only those positions in the short α-helical region of the C-terminal heptad repeats affect the ability of the S glycoprotein to mediate receptor-dependent cell–cell fusion. These findings are consistent with the role of α-helical packing interactions in promoting SARS-CoV S glycoprotein-mediated membrane fusion.

Results

The crystal structure of the six-helix bundle core of the SARS-CoV S glycoprotein contains an extended central trimeric coiled coil of N-terminal heptad-repeat sequences and distinctly shorter C-terminal helices that are limited to two central heptad-repeat units within the longer heptad-repeat sequence (see Fig. 1). To assess the role of this six-helix structure in promoting membrane fusion, we subjected the C-terminal heptad-repeat region of the S glycoprotein from the Urbani isolate of SARS-CoV (Ksiazek et al., 2003) to scanning mutagenesis. Specifically, we focused on residues at ***a*** and ***d*** positions in the heptad repeats, as these hydrophobic sidechains contribute to interhelical knob-in-hole packing interactions that play a dominant role in stabilizing coiled-coil structures (Crick, 1953). These amino acids were individually replaced with serine, a polar residue that would be expected to disturb hydrophobic packing interactions while retaining good α-helix propensity (Chakrabartty et al., 1994). Previous studies of the murine coronavirus S glycoprotein suggested that less severe substitutions with individual alanine residues, a small

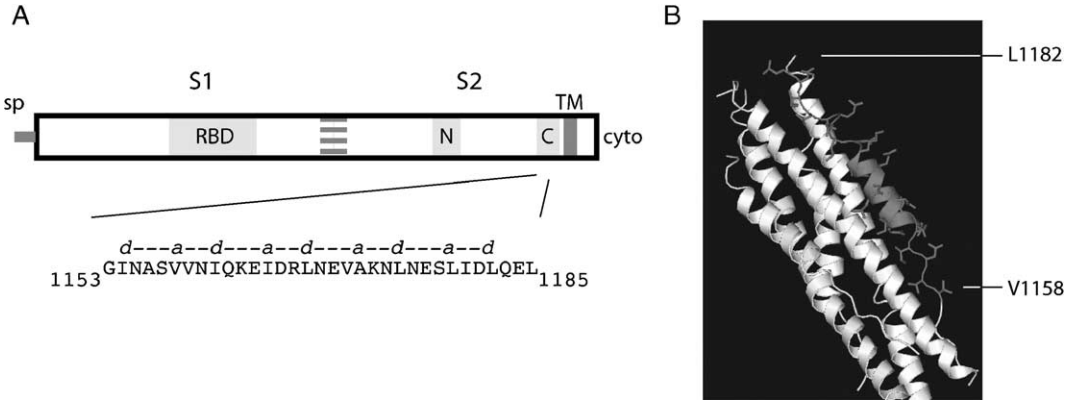

Fig. 1. SARS-CoV S glycoprotein and six-helix bundle. (A) Schematic drawing of S glycoprotein including S1 and S2 domains and the N- and C-terminal heptad-repeat regions. The C-terminal heptad-repeat region is expanded to show the amino acid sequence and the repeating hydrophobic ***a*** and ***d*** positions. Our analysis spans residues V1158 through L1182. Other landmarks include the signal peptide (sp), the receptor-binding domain (RBD) in S1, and the transmembrane (TM) and cytoplasmic (cyto) domains in S2. Sequence homology was used to approximate the location of the S1–S2 boundary, as the furin protease recognition site that is cleaved in Group 2 coronaviruses to form discrete S1 and S2 subunits is absent in the SARS-CoV S glycoprotein (see Discussion). (B) Rendering of the six-helix bundle structure from reference (Xu et al., 2004b) (PDB number 1WNC). One C-terminal chain is highlighted in gray. The helical region is shown in cartoon form and residues included within the heptad repeats are shown as sidechains.

helix-forming amino acid that contributes minimally to hydrophobicity, were insufficient to disrupt six-helix bundle packing (Luo et al., 1999).

Expression of the wild-type and mutant SARS-CoV S glycoproteins in simian COS-7 cells was obtained by transient transfection and was driven by the recombinant vTF7-3 vaccinia virus T7 RNA polymerase (Fuerst et al., 1986). Metabolically labeled cells were lysed in cold Tris–saline buffer containing 1% Triton X-100, and S glycoproteins were isolated via an S-peptide (Spep) affinity tag (Kim and Raines, 1993) at the cytoplasmic C-terminus and S-protein agarose (Novagen). The Spep addition is innocuous with regard to S glycoprotein-mediated membrane fusion (not shown), in keeping with reports of other C-terminal tags (Bisht et al., 2004; Bosch et al., 2004; Moore et al., 2004). The glycoproteins were then eluted in NuPAGE sample buffer (Invitrogen) containing lithium dodecyl sulfate (LDS) and reducing agent and resolved using NuPAGE 3–8% Tris–acetate gels. As shown in Fig. 2, each of the wild-type and mutant glycoproteins was expressed to yield the terminally glycosylated glycoprotein of approximately 220 kDa molecular weight, as well as an immature, Endo H-sensitive form of 200 kDa (Bisht et al., 2004; Song et al., 2004 and K.E.F. and J.H.N, unpublished). The 220-kDa form of the mutant S glycoproteins appeared to migrate somewhat slower than that of the wild type, suggesting a subtle change in terminal glycosylation. Upon deglycosylation with peptide:*N*-glycosidase F (New England BioLabs), all migrated uniformly at the expected 140-kDa molecular weight of the S polypeptide (not shown). As has been reported by others (Bisht et al., 2004; Simmons et al., 2004; Song et al., 2004; Xiao et al., 2003), we found no evidence of proteolytic maturation of the SARS-CoV S glycoprotein to form discrete S1 and S2 subunits. Expression levels of all the mutant S glycoproteins were generally similar to the wild type, with the exception of A1172S, which was reduced. Higher molecular-weight forms of the glycoproteins were also observed to variable degrees among the wild-type and mutant samples (Fig. 2 and below).

Transport of the S glycoproteins to the cell surface was determined by flow cytometry using the SARS-CoV neutralizing MAb F26G18 (Berry et al., 2004) and was found to be unperturbed in all the mutants, including A1172S (Fig. 3). Cell-surface binding of the mutant glycoproteins by other S glycoprotein-directed MAbs (viz., F26G6, F26G8, and F26G19; Berry et al., 2004) was also similar to that of the wild type (not shown). These four MAbs recognize predominantly linear epitopes in the S1 domain (Berry et al., 2004; K.E.F. and J.H.N, unpublished), and thus binding reflects the amount of cell-surface glycoprotein more so than its conformational integrity. Nonetheless, the consistency in cell-surface fluorescence is suggestive of similar transport and presentation. Taken together, these data indicate that none of the serine substitutions markedly affected the biosynthesis or transport to the cell surface of the mutant S glycoproteins.

The ability of the wild-type and mutant S glycoproteins to mediate membrane fusion was assessed by cell–cell fusion using the recombinant vaccinia virus-based β-galactosidase fusion reporter assay (Nussbaum et al., 1994). COS-7 cells expressing the S glycoproteins were co-cultured with COS-7 cells expressing the cell surface receptor of the SARS-CoV, angiotensin converting enzyme 2 (ACE2) (Li et al., 2003). Cell–cell fusion was detected by the induced expression in syncytia of the β-galactosidase reporter. Cell–cell fusion by the wild-type and mutant S

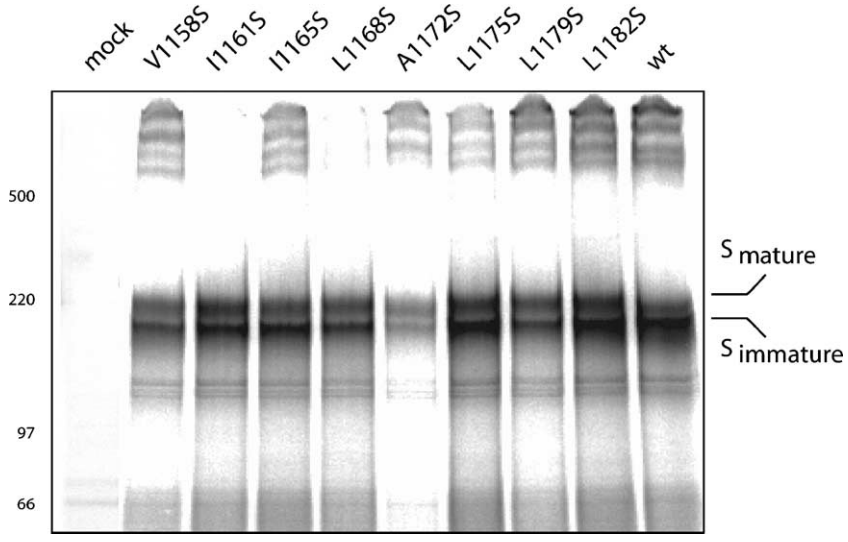

Fig. 2. Expression of wild-type and mutant S glycoproteins. The metabolically labeled S glycoproteins were affinity isolated and separated using NuPAGE 3–8% Tris–acetate gels (Invitrogen). Samples were heated to 70 °C in sample buffer containing LDS and reducing agent prior to electrophoresis. Fixed and dried gels were visualized using a Fuji-3000G Phosphorimager. Rainbow [^{14}C]-molecular weight markers (Amersham Pharmacia Biotech) and the 500-kDa HiMark standard (Invitrogen) are indicated. The mature and immature glycoforms of the S glycoprotein are evident, as are very high molecular-weight species. Identical patterns were obtained using the untagged S glycoprotein and immunoprecipitation by MAbs directed to the S1 domain (not shown).

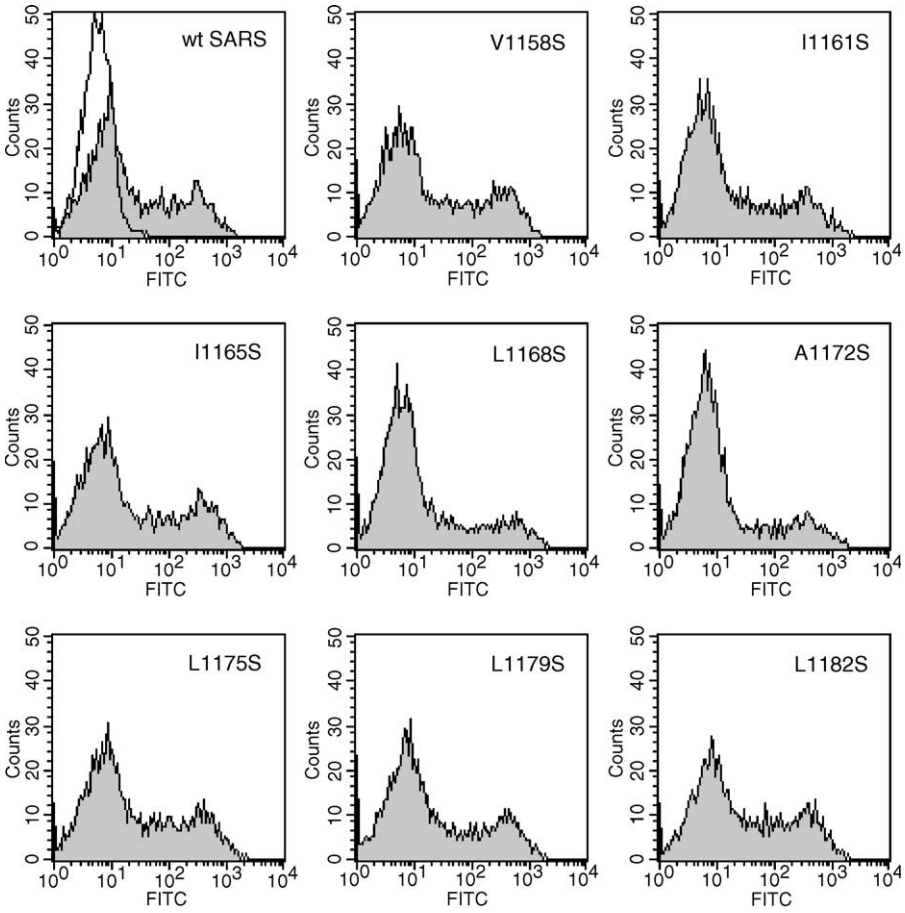

Fig. 3. Flow cytometric analysis of cell surface S glycoprotein. COS-7 cells transiently expressing the wild-type and mutants glycoproteins were stained using the SARS-CoV-neutralizing MAb F26G18 and a secondary fluorescein isothiocyanate (FITC)-conjugated anti-mouse antibody. Cells were analyzed using a FACSCalibur flow cytometer (BD Biosciences), and propidium iodide-staining (dead) cells were excluded. Background staining of mock-transfected cells is shown in the first panel by the open histogram; non-expressing cells are also evident in all transfected cell populations. Expressing cells were defined using a gate of ≥30 (<0.1% of the mock-transfected population). Although the percentages of expressing cells varied (15–30%) with transfection efficiencies, the median fluorescence intensities in all expressing populations were similar (range = 140–180 fluorescence channel).

glycoproteins was entirely dependent on expression of the ACE2 receptor (not shown; Li et al., 2003; Xiao et al., 2003). In these experiments, the ability of the S glycoproteins to mediate ACE2-dependent cell–cell fusion varied markedly among the mutants (Fig. 4A). Substitutions at the termini of the heptad-repeat region had no effect on fusogenicity (viz. V1158S, L1179S, and L1182S) whereas more centrally located substitutions produced variable deficiencies ranging from 10% of wild-type activity (for L1168S) to ≈40% of wild-type activity (for I1161S and A1172S).

Interestingly, all the amino acids identified as important for cell–cell fusion in this analysis lie within the short C-terminal α-helix; these ***a*** and ***d*** position sidechains pack directly into the hydrophobic grooves of the N-terminal coiled coil (Fig. 4B). In the crystal structure, the outlying residues (V1158S, L1179S, and L1182S) exist in an extended non-α-helical conformation of O-X-O repeats (Duquerroy et al., 2005; Ingallinella et al., 2004; Supekar et al., 2004; Xu et al., 2004b) and are not positioned to interact in a conventional knob-into-hole manner with the N-terminal coiled coil. Instead, both V1158 and L1179 utilize main-chain atoms to interact with asparagine and glutamine sidechains on the N-terminal coiled coil (Duquerroy et al., 2005). These interactions are likely undisturbed in the mutant glycoproteins. The convergence between the crystallographic structure of the six-helix bundle and those sidechains critical for membrane fusion provides strong evidence for the central importance of the α-helical bundle in SARS-CoV S glycoprotein-mediated membrane fusion.

It is likely that serine substitutions that affect S glycoprotein-mediated membrane fusion (I1161S, I1165S, L1168S, A1172S, and L1175S) act, in part, by destabilizing the six-helix bundle. Support for this conjecture may be gleaned from an analysis of the higher molecular-weight forms of the S glycoprotein (>500 kDa) shown in Fig. 2. These aggregates are stable at 70 °C to disulfide-bond reduction and LDS denaturation and vary in a consistent manner in the extent of their formation. In appearance and stability, these higher molecular-weight forms are reminis-

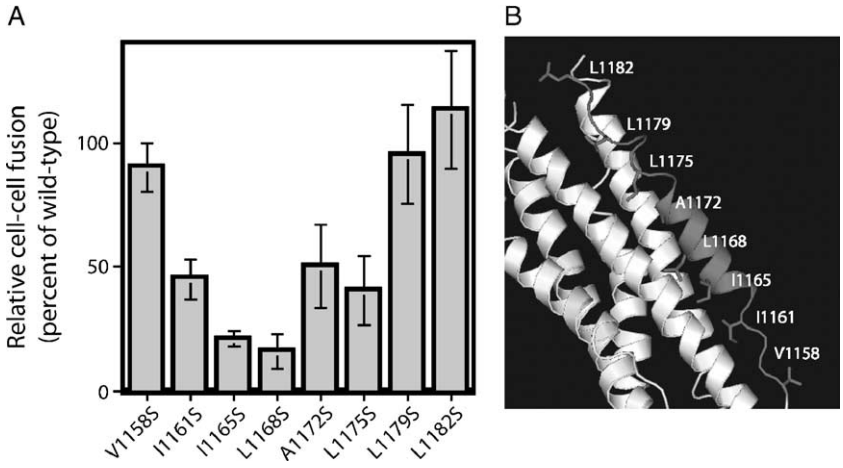

Fig. 4. Fusogenicity of wild-type and mutant S glycoproteins. (A) The ability of the S glycoproteins to promote ACE2-dependent cell–cell fusion was detected using the recombinant vaccinia virus-based β-galactosidase-reporter assay (Nussbaum et al., 1994; York et al., 2004). The number of blue syncytia relative to that in the wild-type S glycoprotein control is shown from two independent experiments, each performed in duplicate; standard deviation is shown as error bars. Transfection efficiencies were comparable in all cases within each experiment. (B) The rendering in Fig. 1 has been annotated to illustrate critical ***a*** and ***d*** heptad-repeat positions relative to the α-helical region.

cent of the fusion-active oligomers of the avian leukosis retrovirus envelope glycoprotein that are induced upon receptor binding and acidic pH (Matsuyama et al., 2004; Mothes et al., 2000; Netter et al., 2004; Smith et al., 2004). Formation of such oligomers may also be triggered by non-physiological means, such as by treatment with nonionic detergent, heat, urea, or guanidium hydrochloride (Carr et al., 1997; Ruigrok et al., 1986; Wallin et al., 2004, 2005). It is possible then that the higher molecular-weight forms observed in the SARS-CoV S glycoprotein represent post-fusion oligomers that provide a fortuitous measure of the relative stability of the wild-type and mutant six-helix bundles. In many of the fusion-deficient S glycoproteins (viz., I1161S, L1168S, A1172S, and L1175S), mutations that affect fusogenicity also affect the extent of formation (Fig. 2) and the thermal stability (not shown) of the higher molecular-weight forms. If borne out in biophysical studies, this interpretation lends additional support to the concept that the formation and stability of the six-helix bundle is intimately coupled to membrane fusion. The I1165S mutant in which fusogenicity is diminished despite the ample formation of the higher molecular-weight species suggests that other parameters may also be important.

Discussion

Our conclusions confirm and extend pioneering findings in another coronavirus species, the prototype murine hepatitis coronavirus (MHV) (Luo et al., 1999). In that work, ***d*** positions in the C-terminal heptad repeats were replaced by alanine. Although single alanine substitutions were insufficient to affect cell–cell fusion, double mutations were highly detrimental and these clustered specifically to the central heptad repeats, and not to the outlying repeats. There too, oligomer formation (as determined by sucrose gradient analysis) correlated with fusogenicity. Translating these early results to the recently determined structure of the MHV six-helix bundle (Xu et al., 2004a), which also reveals a short C-terminal helical region, confirms the notion that the α-helix bundle is an important determinant of S glycoprotein-mediated cell–cell fusion and, by extension, critical for viral entry.

Despite the central role of the six-helix bundle structure in promoting membrane fusion, the family of coronaviruses displays an unusual dimorphism in the length of its N- and C-terminal heptad-repeat regions. Coronaviruses that cluster within one serological and phylogenetic grouping, the Group 1 viruses that include the human respiratory isolate 229E and the feline infectious peritonitis virus (FIPV), contain two additional heptad repeats (14 amino acids) at the center of both N- and C-terminal heptad-repeat regions (Supekar et al., 2004; Xu et al., 2004b). It is likely that these inserts extend and increase the stability of the helical regions in these viruses, but biophysical and structural evidence for this suggestion is currently lacking. Interestingly, the S glycoproteins of established coronaviruses that contain the shorter heptad-repeat regions, specifically the Group 2 coronaviruses that include MHV and the bovine CoV, normally undergo proteolytic maturation during biosynthesis to form discrete receptor-binding (S1) and fusion (S2) subunits (Lai and Holmes, 2001). By contrast, the S glycoproteins of the Group 1 coronaviruses encoding the expanded heptad-repeat regions are not subjected to proteolytic cleavage. Although the newly emerged SARS-CoV encodes the shorter heptad-repeat regions and has been phylogenetically associated with the Group 2 coronavirus (Gibbs et al., 2004; Snijder et al., 2003), its S glycoprotein does not undergo proteolytic maturation. It is unknown what, if any, relationship exists in the coronaviruses between proteolytic cleavage, activation of the structural reorganization in the S glycoprotein, and formation of the six-helix bundle. The seemingly mixed

provenance of the SARS-CoV may have important implications for coronavirus evolution and pathogenesis.

Materials and methods

Molecular reagents and monoclonal antibodies

The S glycoprotein gene of the Urbani isolate of SARS-CoV (Ksiazek et al., 2003) was obtained from P. Rota (Centers for Disease Control and Prevention, Atlanta) and adapted for expression in pcDNA3.1$^-$(Invitrogen). We further modified this plasmid to introduce an S-peptide (Spep) affinity tag (Kim and Raines, 1993) at the cytoplasmic C-terminus of the S glycoprotein to facilitate manipulations. Serine mutations at ***a*** and ***d*** positions of the C-terminal S2 domain heptad repeats (Fig. 1) were introduced by using QuikChange mutagenesis (Stratagene) and confirmed by DNA sequencing. A plasmid expressing the cell surface receptor of the SARS-CoV, angiotensin converting enzyme 2 (ACE2), was kindly provided by M. Farzan (Harvard Medical School, Boston) (Li et al., 2003). Mouse monoclonal antibodies (MAbs) directed to the S glycoprotein were kindly provided by J. Berry (National Center for Foreign Animal Diseases and University of Manitoba, Winnipeg, Canada) (Berry et al., 2004; Gubbins et al., 2005).

Expression of the S glycoprotein

The full-length S glycoprotein was transiently expressed in COS-7 cells using the pcDNA3.1$^-$ T7 promoter and the recombinant vaccinia virus vTF7-3 encoding T7 polymerase (Fuerst et al., 1986). vTF7-3 was obtained from T. Fuerst and B. Moss (National Institutes of Health) through the NIH AIDS Research and Reference Reagent Program. COS-7 cells were infected with the recombinant vaccinia virus at a multiplicity of eight in Dulbecco's Minimal Essential Medium (DMEM) containing 2% fetal bovine serum (FBS). Cytosine arabinoside (araC) was included at 10 μM to limit vaccinia virus expression (Hruby et al., 1980). After 30 min, the cells were washed and transfected with the S glycoprotein-expression plasmid using FuGene-6 reagent (Roche Biochemicals). Metabolic labeling using 50 μCi/ml of [^{35}S]-ProMix (Amersham Pharmacia Biotech) was initiated 6 h post-transfection in methionine- and cysteine-free DMEM containing 10% dialyzed FBS and 10 μM araC, and was continued for 12–16 h. Cultures were then washed in physiological buffered saline (PBS) and lysed using cold Tris–saline buffer (50 mM Tris–HCl and 150 mM NaCl at pH 7.5) containing 1% Triton X-100 nonionic detergent and protease inhibitors (1 μg/ml each of aprotinin, leupeptin, and pepstatin). A soluble fraction was prepared by centrifugation at 15,000×*g* for 30 min at 4 °C. The expressed S glycoproteins were isolated using the Spep affinity tag and S-protein agarose (Novagen) and resolved using NuPAGE 3–8% Tris–acetate gels (Invitrogen) and the recommended sample buffer containing LDS and reducing agent. Samples were heated to 70 °C prior to electrophoresis. Molecular weight markers included [^{14}C]-methylated Rainbow proteins (Amersham Pharmacia Biotech) and HiMark standards (Invitrogen). Radiolabeled proteins were imaged using a Fuji FLA-3000G imager and analyzed using ImageGauge software (Fuji).

Flow cytometry

COS-7 cells transiently expressing the wild-type and mutant glycoproteins were labeled using the SARS-CoV-neutralizing MAb F26G18 (Berry et al., 2004) and a secondary fluorescein isothiocyanate (FITC)-conjugated goat anti-mouse antibody (Jackson ImmunoResearch). Cells were subsequently stained using propidium iodide (1 μg/ml) and then fixed in 2% formaldehyde. Populations were analyzed using a FACSCalibur flow cytometer and CellQuest software (BD Biosciences).

S glycoprotein-mediated cell–cell fusion

The β-galactosidase fusion reporter assay (Nussbaum et al., 1994) was used to assess the ability of the wild-type and mutant S glycoproteins to mediate receptor-dependent cell–cell fusion. The recombinant vaccinia virus vCB21R-lacZ expressing β-galactosidase under the control of the T7 promoter (Nussbaum et al., 1994) was obtained from C. Broder, P. Kennedy, and E. Berger (NIH) through the AIDS Research and Reference Reagent Program. In these studies, COS-7 cells infected with vTF7-3 and expressing the S glycoprotein were co-cultured with COS-7 cells transfected to express the SARS-CoV cellular receptor ACE2 (Li et al., 2003) and infected with vCB21R-lacZ. β-galactosidase expression is induced upon fusion of the effector and target cells (Nussbaum et al., 1994). To generate the target cell population, COS-7 cells that had been transfected one day previously with the ACE2-expression plasmid (Li et al., 2003) were incubated with vCB21R-lacZ at a multiplicity of 10 and the infection was allowed to proceed overnight in the presence of 100 μg/ml of the vaccinia virus assembly inhibitor, rifampicin. The following day, S glycoprotein-expressing cells and ACE2-expressing target cells were co-cultured for 10 h in medium containing both araC and rifampicin (Hruby et al., 1980; York et al., 2004). Cultures were then fixed for 5 min at 4 °C in cold PBS containing 2% formaldehyde and 0.2% glutaraldehyde, and β-galactosidase activity was detected using the chromogenic X-gal substrate (Nussbaum et al., 1994). The numbers of blue syncytia were determined microscopically.

Acknowledgments

We thank Drs. Paul Rota (Centers for Disease Control and Prevention, Atlanta), Jody Berry (National Center for

Foreign Animal Diseases and University of Manitoba, Winnipeg, Canada), and Michael Farzan (Harvard Medical School, Boston) for graciously providing recently developed reagents for this work. J.H.N. is grateful to Drs. Min Lu (Weill Medical College of Cornell University, New York) and Meg Trahey (The University of Montana) for helpful discussions during the course of the work and in preparation of the manuscript. We thank Kimberly Hardwick for technical assistance in generating mutants.

References

Berry, J.D., Jones, S., Drebot, M.A., Andonov, A., Sabara, M., Yuan, X.Y., Weingartl, H., Fernando, L., Marszal, P., Gren, J., Nicolas, B., Andonova, M., Ranada, F., Gubbins, M.J., Ball, T.B., Kitching, P., Li, Y., Kabani, A., Plummer, F., 2004. Development and characterisation of neutralising monoclonal antibody to the SARS-coronavirus. J. Virol. Methods 120, 87–96.

Bisht, H., Roberts, A., Vogel, L., Bukreyev, A., Collins, P.L., Murphy, B.R., Subbarao, K., Moss, B., 2004. Severe acute respiratory syndrome coronavirus spike protein expressed by attenuated vaccinia virus protectively immunizes mice. Proc. Natl. Acad. Sci. U.S.A. 101, 6641–6646.

Bosch, B.J., van der Zee, R., de Haan, C.A., Rottier, P.J., 2003. The coronavirus spike protein is a class I virus fusion protein: structural and functional characterization of the fusion core complex. J. Virol. 77, 8801–8811.

Bosch, B.J., de Haan, C.A., Rottier, P.J., 2004. Coronavirus spike glycoprotein, extended at the carboxy terminus with green fluorescent protein, is assembly competent. J. Virol. 78, 7369–7378.

Carr, C.M., Chaudhry, C., Kim, P.S., 1997. Influenza hemagglutinin is spring-loaded by a metastable native conformation. Proc. Natl. Acad. Sci. U.S.A. 94, 14306–14313.

Chakrabartty, A., Kortemme, T., Baldwin, R.L., 1994. Helix propensities of the amino acids measured in alanine-based peptides without helix-stabilizing side-chain interactions. Protein Sci. 3, 843–852.

Chambers, P., Pringle, C.R., Easton, A.J., 1990. Heptad repeat sequences are located adjacent to hydrophobic regions in several types of virus fusion glycoproteins. J. Gen. Virol. 71, 3075–3080.

Crick, F.H.C., 1953. The packing of α-helices: simple coiled coils. Acta Crystallogr. 6, 689–697.

Drosten, C., Gunther, S., Preiser, W., van der Werf, S., Brodt, H.R., Becker, S., Rabenau, H., Panning, M., Kolesnikova, L., Fouchier, R.A., Berger, A., Burguiere, A.M., Cinatl, J., Eickmann, M., Escriou, N., Grywna, K., Kramme, S., Manuguerra, J.C., Muller, S., Rickerts, V., Sturmer, M., Vieth, S., Klenk, H.D., Osterhaus, A.D., Schmitz, H., Doerr, H.W., 2003. Identification of a novel coronavirus in patients with severe acute respiratory syndrome. N. Engl. J. Med. 348, 1967–1976.

Duquerroy, S., Vigouroux, A., Rottier, P.J., Rey, F.A., Bosch, J.B., 2005. Central ions and lateral asparagine/glutamine zippers stabilize the post-fusion hairpin conformation of the SARS coronavirus spike glycoprotein. Virology 335, 276–285.

Eckert, D.M., Kim, P.S., 2001. Mechanisms of viral membrane fusion and its inhibition. Annu. Rev. Biochem. 70, 777–810.

Fuerst, T.R., Niles, E.G., Studier, F.W., Moss, B., 1986. Eukaryotic transient-expression system based on recombinant vaccinia virus that synthesizes bacteriophage T7 RNA polymerase. Proc. Natl. Acad. Sci. U.S.A. 83, 8122–8126.

Gibbs, A.J., Gibbs, M.J., Armstrong, J.S., 2004. The phylogeny of SARS coronavirus. Arch. Virol. 149, 621–624.

Gubbins, M.J., Plummer, F.A., Yuan, X.Y., Johnstone, D., Drebot, M., Andonova, M., Andonov, A., Berry, J.D., 2005. Molecular characterization of a panel of murine monoclonal antibodies specific for the SARS-coronavirus. Mol. Immunol. 42, 125–136.

Hruby, D.E., Lynn, D.L., Kates, J.R., 1980. Identification of a virus-specified protein in the nucleus of vaccinia virus-infected cells. J. Gen. Virol. 47, 293–299.

Hughson, F.M., 1997. Enveloped viruses: a common mode of membrane fusion? Curr. Biol. 7, R565–R569.

Ingallinella, P., Bianchi, E., Finotto, M., Cantoni, G., Eckert, D.M., Supekar, V.M., Bruckmann, C., Carfi, A., Pessi, A., 2004. Structural characterization of the fusion–active complex of severe acute respiratory syndrome (SARS) coronavirus. Proc. Natl. Acad. Sci. U.S.A. 101, 8709–8714.

Kim, J.-S., Raines, R.T., 1993. Ribonuclease S-peptide as a carrier in fusion proteins. Protein Sci. 2, 348–356.

Ksiazek, T.G., Erdman, D., Goldsmith, C.S., Zaki, S.R., Peret, T., Emery, S., Tong, S., Urbani, C., Comer, J.A., Lim, W., Rollin, P.E., Dowell, S.F., Ling, A.E., Humphrey, C.D., Shieh, W.J., Guarner, J., Paddock, C.D., Rota, P., Fields, B., DeRisi, J., Yang, J.Y., Cox, N., Hughes, J.M., LeDuc, J.W., Bellini, W.J., Anderson, L.J., SARS Working Group, 2003. A novel coronavirus associated with severe acute respiratory syndrome. N. Engl. J. Med. 348, 1953–1966.

Kuiken, T., Fouchier, R.A., Schutten, M., Rimmelzwaan, G.F., van Amerongen, G., van Riel, D., Laman, J.D., de Jong, T., van Doornum, G., Lim, W., Ling, A.E., Chan, P.K., Tam, J.S., Zambon, M.C., Gopal, R., Drosten, C., van der Werf, S., Escriou, N., Manuguerra, J.C., Stohr, K., Peiris, J.S., Osterhaus, A.D., 2003. Newly discovered coronavirus as the primary cause of severe acute respiratory syndrome. Lancet 362, 263–270.

Lai, M.M.C., Holmes, K.V., 2001. Coronaviridae: the viruses and their replication. In: Knipe, D., Howley, P.M. (Eds.), Fields' Virology, 4th ed. Lippincott Williams and Wilkins, Philadelphia, pp. 1163–1185.

Li, W., Moore, M.J., Vasilieva, N., Sui, J., Wong, S.K., Berne, M.A., Somasundaran, M., Sullivan, J.L., Luzuriaga, K., Greenough, T.C., Choe, H., Farzan, M., 2003. Angiotensin-converting enzyme 2 is a functional receptor for the SARS coronavirus. Nature 426, 450–454.

Liu, S., Xiao, G., Chen, Y., He, Y., Niu, J., Escalante, C.R., Xiong, H., Farmar, J., Debnath, A.K., Tien, P., Jiang, S., 2004. Interaction between heptad repeat 1 and 2 regions in spike protein of SARS-associated coronavirus: implications for virus fusogenic mechanism and identification of fusion inhibitors. Lancet 363, 938–947.

Luo, Z., Matthews, A.M., Weiss, S.R., 1999. Amino acid substitutions within the leucine zipper domain of the murine coronavirus spike protein cause defects in oligomerization and the ability to induce cell-to-cell fusion. J. Virol. 73, 8152–8159.

Marra, M.A., Jones, S.J., Astell, C.R., Holt, R.A., Brooks-Wilson, A., Butterfield, Y.S., Khattra, J., Asano, J.K., Barber, S.A., Chan, S.Y., Cloutier, A., Coughlin, S.M., Freeman, D., Girn, N., Griffith, O.L., Leach, S.R., Mayo, M., McDonald, H., Montgomery, S.B., Pandoh, P.K., Petrescu, A.S., Robertson, A.G., Schein, J.E., Siddiqui, A., Smailus, D.E., Stott, J.M., Yang, G.S., Plummer, F., Andonov, A., Artsob, H., Bastien, N., Bernard, K., Booth, T.F., Bowness, D., Czub, M., Drebot, M., Fernando, L., Flick, R., Garbutt, M., Gray, M., Grolla, A., Jones, S., Feldmann, H., Meyers, A., Kabani, A., Li, Y., Normand, S., Stroher, U., Tipples, G.A., Tyler, S., Vogrig, R., Ward, D., Watson, B., Brunham, R.C., Krajden, M., Petric, M., Skowronski, D.M., Upton, C., Roper, R.L., 2003. The genome sequence of the SARS-associated coronavirus. Science 300, 1399–1440.

Matsuyama, S., Delos, S.E., White, J.M., 2004. Sequential roles of receptor binding and low pH in forming prehairpin and hairpin conformations of a retroviral envelope glycoprotein. J. Virol. 78, 8201–8209.

Moore, M.J., Dorfman, T., Li, W., Wong, S.K., Li, Y., Kuhn, J.H., Coderre, J., Vasilieva, N., Han, Z., Greenough, T.C., Farzan, M., Choe, H., 2004. Retroviruses pseudotyped with the severe acute respiratory syndrome coronavirus spike protein efficiently infect cells expressing angiotensin-converting enzyme 2. J. Virol. 78, 10628–10635.

Mothes, W., Boerger, A.L., Narayan, S., Cunningham, J.M., Young, J.A., 2000. Retroviral entry mediated by receptor priming and low pH triggering of an envelope glycoprotein. Cell 103, 679–689.

Netter, R.C., Amberg, S.M., Balliet, J.W., Biscone, M.J., Vermeulen, A.,

Earp, L.J., White, J.M., Bates, P., 2004. Heptad repeat 2-based peptides inhibit avian sarcoma and leukosis virus subgroup a infection and identify a fusion intermediate. J. Virol. 78, 13430–13439.

Nussbaum, O., Broder, C.C., Berger, E.A., 1994. Fusogenic mechanisms of enveloped-virus glycoproteins analyzed by a novel recombinant vaccinia virus-based assay quantitating cell fusion-dependent reporter gene activation. J. Virol. 68, 5411–5422.

Peiris, J.S., Lai, S.T., Poon, L.L., Guan, Y., Yam, L.Y., Lim, W., Nicholls, J., Yee, W.K., Yan, W.W., Cheung, M.T., Cheng, V.C., Chan, K.H., Tsang, D.N., Yung, R.W., Ng, T.K., Yuen, K.Y., SARS study group, 2003. Coronavirus as a possible cause of severe acute respiratory syndrome. Lancet 361, 1319–1325.

Rota, P.A., Oberste, M.S., Monroe, S.S., Nix, W.A., Campagnoli, R., Icenogle, J.P., Penaranda, S., Bankamp, B., Maher, K., Chen, M.H., Tong, S., Tamin, A., Lowe, L., Frace, M., DeRisi, J.L., Chen, Q., Wang, D., Erdman, D.D., Peret, T.C., Burns, C., Ksiazek, T.G., Rollin, P.E., Sanchez, A., Liffick, S., Holloway, B., Limor, J., McCaustland, K., Olsen-Rasmussen, M., Fouchier, R., Gunther, S., Osterhaus, A.D., Drosten, C., Pallansch, M.A., Anderson, L.J., Bellini, W.J., 2003. Characterization of a novel coronavirus associated with severe acute respiratory syndrome. Science 300, 1394–1399.

Ruigrok, R.W., Martin, S.R., Wharton, S.A., Skehel, J.J., Bayley, P.M., Wiley, D.C., 1986. Conformational changes in the hemagglutinin of influenza virus which accompany heat-induced fusion of virus with liposomes. Virology 155, 484–497.

Simmons, G., Reeves, J.D., Rennekamp, A.J., Amberg, S.M., Piefer, A.J., Bates, P., 2004. Characterization of severe acute respiratory syndrome-associated coronavirus (SARS-CoV) spike glycoprotein-mediated viral entry. Proc. Natl. Acad. Sci. U.S.A. 101, 4240–4245.

Skehel, J.J., Wiley, D.C., 2000. Receptor binding and membrane fusion in virus entry: the influenza hemagglutinin. Annu. Rev. Biochem. 69, 531–569.

Smith, J.G., Mothes, W., Blacklow, S.C., Cunningham, J.M., 2004. The mature avian leukosis virus subgroup A envelope glycoprotein is metastable, and refolding induced by the synergistic effects of receptor binding and low pH is coupled to infection. J. Virol. 78, 1403–1410.

Snijder, E.J., Bredenbeek, P.J., Dobbe, J.C., Thiel, V., Ziebuhr, J., Poon, L.L., Guan, Y., Rozanov, M., Spaan, W.J., Gorbalenya, A.E., 2003. Unique and conserved features of genome and proteome of SARS-coronavirus, an early split-off from the coronavirus group 2 lineage. J. Mol. Biol. 331, 991–1004.

Song, H.C., Seo, M.Y., Stadler, K., Yoo, B.J., Choo, Q.L., Coates, S.R., Uematsu, Y., Harada, T., Greer, C.E., Polo, J.M., Pileri, P., Eickmann, M., Rappuoli, R., Abrignani, S., Houghton, M., Han, J.H., 2004. Synthesis and characterization of a native, oligomeric form of recombinant severe acute respiratory syndrome coronavirus spike glycoprotein. J. Virol. 78, 10328–10335.

Supekar, V.M., Bruckmann, C., Ingallinella, P., Bianchi, E., Pessi, A., Carfi, A., 2004. Structure of a proteolytically resistant core from the severe acute respiratory syndrome coronavirus S2 fusion protein. Proc. Natl. Acad. Sci. U.S.A. 101, 17958–17963.

Tripet, B., Howard, M.W., Jobling, M., Holmes, R.K., Holmes, K.V., Hodges, R.S., 2004. Structural characterization of the SARS-coronavirus spike S fusion protein core. J. Biol. Chem. 279, 20836–20849.

Wallin, M., Ekstrom, M., Garoff, H., 2004. Isomerization of the intersubunit disulphide-bond in Env controls retrovirus fusion. EMBO J. 23, 54–65.

Wallin, M., Ekstrom, M., Garoff, H., 2005. The fusion-controlling disulfide bond isomerase in retrovirus Env is triggered by protein destabilization. J. Virol. 79, 1678–1685.

Weissenhorn, W., Dessen, A., Calder, L.J., Harrison, S.C., Skehel, J.J., Wiley, D.C., 1999. Structural basis for membrane fusion by enveloped viruses. Mol. Membr. Biol. 16, 3–9.

Xiao, X., Chakraborti, S., Dimitrov, A.S., Gramatikoff, K., Dimitrov, D.S., 2003. The SARS-CoV S glycoprotein: expression and functional characterization. Biochem. Biophys. Res. Commun. 312, 1159–1164.

Xu, Y., Liu, Y., Lou, Z., Qin, L., Li, X., Bai, Z., Pang, H., Tien, P., Gao, G.F., Rao, Z., 2004a. Structural basis for coronavirus-mediated membrane fusion. Crystal structure of mouse hepatitis virus spike protein fusion core. J. Biol. Chem. 279, 30514–30522.

Xu, Y., Lou, Z., Liu, Y., Pang, H., Tien, P., Gao, G.F., Rao, Z., 2004b. Crystal structure of severe acute respiratory syndrome coronavirus spike protein fusion core. J. Biol. Chem. 279, 49414–49419.

York, J., Romanowski, V., Lu, M., Nunberg, J.H., 2004. The signal peptide of the Junín arenavirus envelope glycoprotein is myristoylated and forms an essential subunit of the mature G1–G2 complex. J. Virol. 78, 10783–10792.